**Fachtagung "Experimentelle Strömungsmechanik"**
3. - 5. September 2024, Berlin

# Einsetzende Partikelbewegung in einer trägheitsbehafteten, laminaren Scherströmung

## Onset of particle motion in inertial laminar shear flow

**S. Wrana[1], C. Näger[1], A. Wierschem[1]**
[1]Lehrstuhl für Strömungsmechanik, Friedrich-Alexander-Universität Erlangen-Nürnberg, Cauerstraße 4, 91058 Erlangen, Germany

Einsetzende Partikelbewegung, Trägheit, laminare Scherströmung
Onset of particle motion, inertia, laminar shear flow

### Abstract

This paper investigates the impact of inertia on the shear-induced onset of particle motion at a regular substrate. To this end, we designed a new experimental setup consisting of a conveyor belt located in a temperature-controlled tank filled with silicone oil. We generate a plane Couette flow between the conveyor belt and the substrate. The substrate consists of 20,000 spherical particles with a diameter of 5 mm in a fixed quadratic arrangement. On top, we place a single mobile bead and capture its movement with a camera. The onset of motion is characterized by the Shields number. The particle Reynolds number ranges from 0.6 to 1.3.

### Introduction

The initiation of particle motion is a critical phenomenon with implications for various natural and industrial processes. It plays an important role in sediment transport in rivers and shorelines, bed erosion, the formation of dunes or ripples, as explored by previous studies (Wierschem et al., 2008; Groh et al., 2008; Carneiro et al., 2011). Additionally, it influences filtration processes, surface cleaning, pneumatic conveying (Stevanovic et al., 2014), particle assembly for meta-materials (Nguyen and Yoon, 2009; Yin et al., 2001; Bleil et al., 2006), and cell detachment (Dakhil et al., 2018). The onset of particle motion has been extensively studied over the past decades, primarily under turbulent flow conditions and on highly disordered substrates (Shields, 1936; White, 1940; Dey and Ali, 2018). While incipient particle motion in laminar flow has been considered in recent years (Charru et al., 2004; Loiseleux, 2005; Derksen, 2001; Seizilles, 2013; Deskus and Diplas, 2018), there remain open issues concerning well-organized substrates under laminar flow conditions. In this study, we investigate the onset of particle motion in a controlled laminar shear flow with a fixed quadratic substrate. This approach enables a more precise determination of the key parameters influencing incipient motion (Agudo and Wierschem, 2012; Agudo et al., 2014; Agudo et al., 2017; Agudo et al. 2018; Topic et al., 2019; Topic et al., 2022). While the prior studies by Wierschem and collaborators analyzed incipient motion under creeping flow conditions on the particle scale, our setup extends the parameter range to include inertial flow conditions with particle Reynolds numbers ranging from 0.5 to around 40, while for the measurements in this study the particle Reynolds number ranges from 0.6 to 1.3.



GALA e.V., Karlsruhe, Germany, ISBN 978-3-9816764-4-0

## Theoretical foundations

To characterize the onset of particle motion, most studies (Agudo and Wierschem, 2012; Agudo et al., 2014; Agudo et al., 2017; Agudo et al. 2018; Topic et al., 2019; Topic et al., 2022, Dey and Ali, 2018) focus on the Shields number, which is defined as the ratio of the flow-induced friction force to the effective particle weight:

$$\theta = \frac{\mu\dot{\gamma}}{\left(\frac{\rho_P}{\rho_F} - 1\right) g D_P} \tag{1}$$

Where $\boldsymbol{\theta}$ is the Shields number, $\boldsymbol{\rho_P}$ the particle density, $\boldsymbol{\rho_F}$ the fluid density, $\boldsymbol{g}$ the acceleration of gravity, $\boldsymbol{D_p}$ the diameter of the single particle, $\boldsymbol{\mu}$ the kinematic viscosity of the silicone oil and $\dot{\boldsymbol{\gamma}}$ the shear rate in the gap created by the belt velocity.

To characterize the flow conditions, we use the Reynolds number $Re$ and for the impact of the fluid on the mobile bead, we use the particle Reynolds number $Re_P$:

$$Re_P = \frac{\dot{\gamma} D_P^2}{\mu} \tag{2}$$

Where the Particle Reynolds number is $\boldsymbol{Re_P}$, the shear rate is $\dot{\boldsymbol{\gamma}}$, the particle diameter is $\boldsymbol{D_P}$ and the kinematic viscosity is $\boldsymbol{\mu}$.

$$Re = Re_P \left(\frac{h}{D_P}\right)^2 \tag{3}$$

Where $\boldsymbol{Re}$ is the Reynolds number, $\boldsymbol{Re_P}$ is the particle Reynolds number, $\boldsymbol{h}$ is the gap height and $\boldsymbol{D_P}$ is the particle diameter.

## Experimental setup

Previous studies by Agudo and Wierschem 2012 and Agudo et al. 2014 at creeping flow conditions have been carried out using a rotational rheometer. However, to investigate the effects of inertia, it is essential to use a linear setup in order to avoid centrifugal forces. Various setups have been employed and tested in the past to study a linear Couette flow (Taylor, 1934; Tillmark and Alfredsson, 1991; Daviaud et al, 1992; Birkhofer et al., 2005; Couliou and Monchaux, 2015). We adapted and implemented a new setup manufactured for our specific requirements. In this setup, a conveyor belt is used to create laminar a Couette flow between the belt and a substrate below, as illustrated in Figure 1.



GALA e.V., Karlsruhe, Germany, ISBN 978-3-9816764-4-0

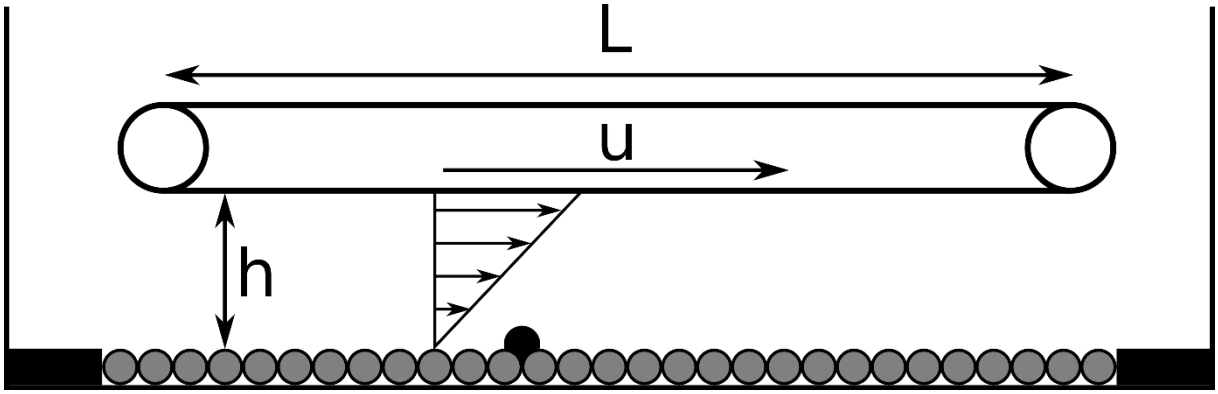


Figure 1: Side view of the experimental setup. L is the length of the belt, h is the gap height and u the belt velocity. The conveyor belt (black) is submerged in silicone oil in the container. At the bottom are the fixed substrate spheres in grey and on top the mobile bead in black.

The conveyor belt is a standard model (Gurtförderer 40 C4N) manufactured by Robotunits GmbH, measuring 2 m in length and 0.25 m in width. The belt itself (E 4/2 U0/U2 MT-HAACCP from siegling transilon) is made of polyester with a polyurethane coating and a total thickness of 1.35 mm and features a smooth surface. It is driven by a computer controlled servomotor EGK80-80NR from Groschopp and its velocity can be adjusted in steps of 1 mm/s up to a maximum velocity of 2.0 m/s.

The container, made of transparent Plexiglas, has dimensions of 2.30 m in length, 0.3 m in height and 0.6 m in width, with dividing sidewall along the belt. This side wall has closable windows allowing access from the side for placing the mobile particles under the belt. The container is filled with silicone oil (Kurt Obermeier GmbH & Co. KG) with a viscosity of 99.86±0.03 $mm^2/s$ at 20 °C and a density of 0.968±0.0005 $g/cm^3$ up to a height of 0.25 m.

The conveyor belt is supported by four lifting spindles, allowing for adjustment of the gap height between the belt and the substrate in increments of 0.1 mm. These spindles rest on the sidewalls of the container and are mounted to aluminum rails that serve as the framework for the setup. The substrate, embedded in a 2.5 cm thick aluminum plate, consists of 20,000 steel spheres (1.4034, grade G20 DIN 5401) with a diameter of 5 mm arranged in a quadratic order, resulting in a test section that is 400 spheres long and 50 spheres wide. To hold the substrate beads in position, the spheres are placed onto a perforated polycarbonate plate with a thickness of 1 mm. Since flow velocities in the substrate grooves and below the substrate spheres are much smaller than above the substrate (Agudo et al., 2017), there is no relevant influence of the plate on the measurement. The mobile bead, that is to be analyzed, is placed onto that substrate. The particle motion is detected with a camera (CMOS HighSpeed Camera pco. 1200) from the side as shown in Figure 2.



GALA e.V., Karlsruhe, Germany, ISBN 978-3-9816764-4-0

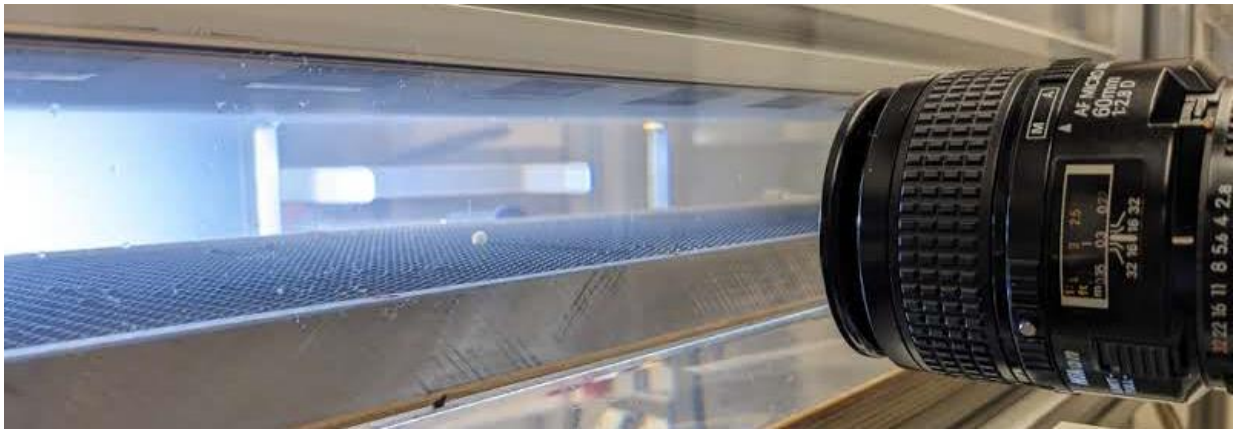

Figure 2: Side view of the flow channel with polyamide bead in the middle and objective lens of the camera on the right.

Embedded within the substrate plate are copper tubes that can be used to regulate the temperature of the silicone oil by circulating tempered water through them. The water temperature can be precisely controlled using a Thermo Haake C25P thermostat. If necessary, the flow channel can be illuminated with an IntraLED 2020 light source.

To extend the parameter range, we vary the gap width, belt velocity, particle density, kinematic viscosity and bead diameter. To vary the particle density, we use beads of different materials (polyamide 6.6, polyoxymethylene, soda-lime glass, silicon nitride and aluminum oxide).

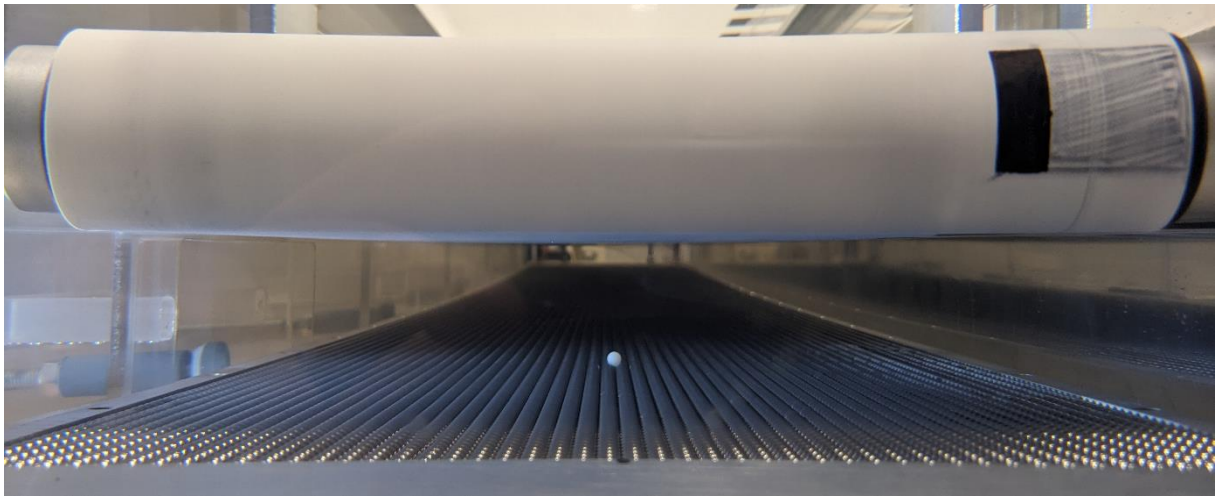
Figure 3: Front view of the flow channel with substrate, mobile bead (white) and conveyor belt above.

In order to protect the setup from vibrations, it is placed on a vibration-damping mat. Furthermore it was essential to verify that the motor adjusted velocity corresponded accurately to the desired belt velocity. Given that our belt is submerged in silicon oil and operates at relatively high velocities, slippage between the driving roller and the belt was a potential concern. To determine the belt velocity, we applied black marks on the white belt and tracked them using two non-contact contrast sensors (BKT0012 from Balluff). These sensors emit a laser beam onto the belt and detect the reflected light, which varies based on the color and thus on the absorption properties of the belt. The belt velocity is determined with the marks by measuring the distance of 16.77±0.03 mm between the two sensors and recording the time taken for a mark to move from one sensor location to the other. We employed two different methods for



GALA e.V., Karlsruhe, Germany, ISBN 978-3-9816764-4-0

deducing the velocity: The first method measures the time taken for a mark to pass both sensors and updates the velocity each time another mark passes by. This approach ensures a high update rate right from the start of the measurement, enabling prompt detection of any small slippage. In the end, the average velocity and the standard derivation of all measurements are calculated. The second method calculates the time taken for a mark to be scanned twice – once upon initial detection and again after completing a full rotation of the belt. While this reduces the initial update rate for the belt velocity, it significantly increases the distance used for the velocity calculation to 4043.5 mm, rendering errors due to uncertainties of the distance measurement negligible.

To ensure the cleanliness of the oil by preventing the presence of dust or dirt particles in the flow, the setup is enclosed and the oil is regularly filtered using a Pulcino 10 oil filter system capable of filtering particles down to 25 µm in size.

**Verification of the desired functionality**

The critical Shields number for incipient particle motion is analyzed at multiple positions on the substrate under varying flow conditions. For each measurement, a mobile bead is positioned in the specified area under desired conditions. Subsequently, the belt velocity is increased in increments of 1 mm/s. The velocity is then recorded for a duration of 40 seconds and the movement of the bead is observed with the camera. If the bead does not start moving within the 40 seconds interval, the velocity is further increased for subsequent trials. The gap height for these measurements was 45 mm and the temperature was kept at 22.3±1.0 °C.

We started this study by examining the in- and outflow conditions to identify the region where the Couette flow is fully developed. To this end, the mobile bead (5 mm, polyamide, GII, DIN5401) was positioned along the centerline of the flow channel, with its location adjusted in intervals of 10 cm along the flow direction. For developed flow, a stable Shields number is expected. As depicted in Figure 4, this is observed between 12.75 cm and 142.75 cm downstream from the inflow of the channel, where the standard deviation among different positions is 2.7 %. This rage is equal to a length of 2.8 to 32 times the gap height. The Reynolds number under these conditions is 48 and the particle Reynolds number is 0.6 with a standard derivation of 2.8 % for both Reynolds numbers. Subsequent measurements will be carried out at position 102.75 cm to ensure minimal influence from the inflow or outflow.



GALA e.V., Karlsruhe, Germany, ISBN 978-3-9816764-4-0

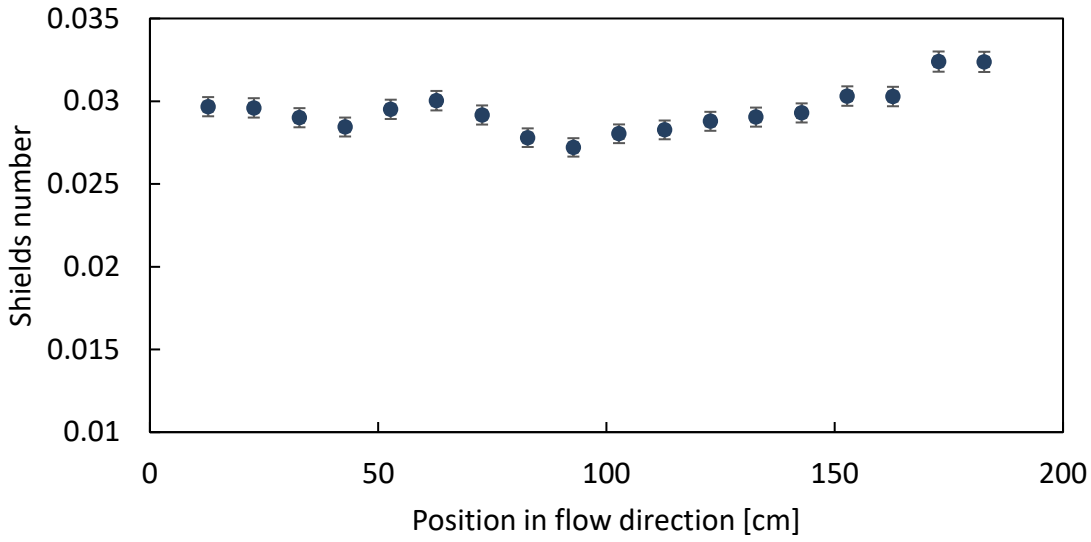


Figure 4: Shields number depending on the position of the bead in flow direction. 0 cm marks the beginning and 200 cm the end of the belt.

Next, the influence of the side walls was examined by adjusting the position of the bead in a direction perpendicular to the flow direction. In Figure 5, it is evident that the impact of the side walls extends into the flow but diminishes rapidly before reaching the central region of the flow channel where the bead is intended to be located. From the middle of the flow channel up to 65 mm to the side, the standard derivation is 2.6 %.

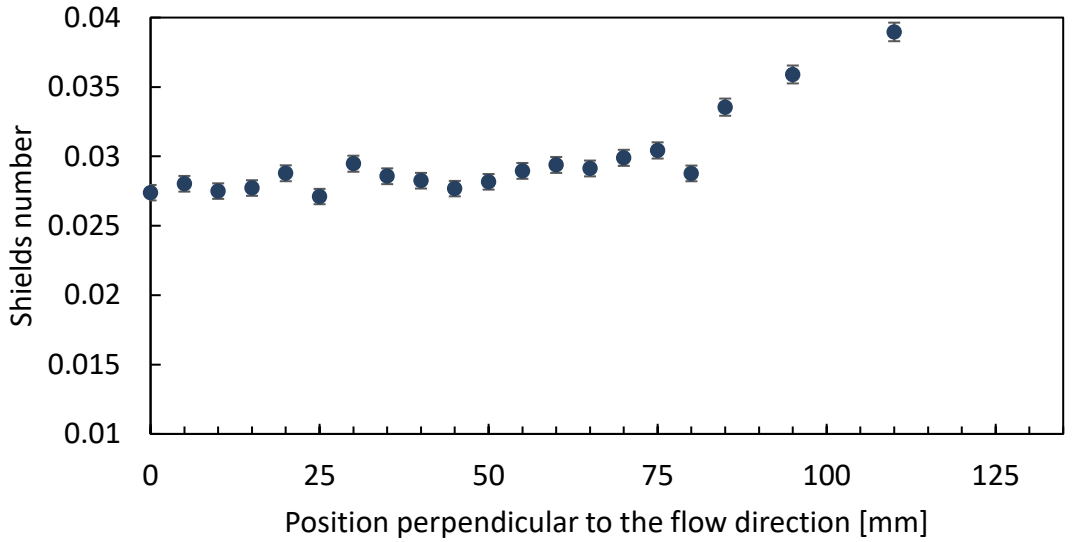


Figure 5: Influence of the side walls on the Shields number. The position at 0 mm is the middle of the flow channel and 135 mm is the side wall of the flow channel. The belt itself and the substrate end at 125 mm.

To analyze the findings presented in Figures 4 and 5, we studied the flow field with particle image velocimetry (PIV). The PIV system, described in more detail by Näger et al., was equipped with a Continuum Terra 527-20m pulsed laser (wavelength: 527 nm). As tracers, we used fluorescent polystyrene particles doped with rhodamine B with an average diameter of 6 µm. The camera (FASTCAM SA-X2) was equipped with a red filter in order to suppress the



GALA e.V., Karlsruhe, Germany, ISBN 978-3-9816764-4-0

green laser light. The data analysis was performed using the software PIVlab. Figure 6 illustrates a close to linear flow profile with a regression coefficient of 0.99 further confirming the attainment of the desired flow conditions.

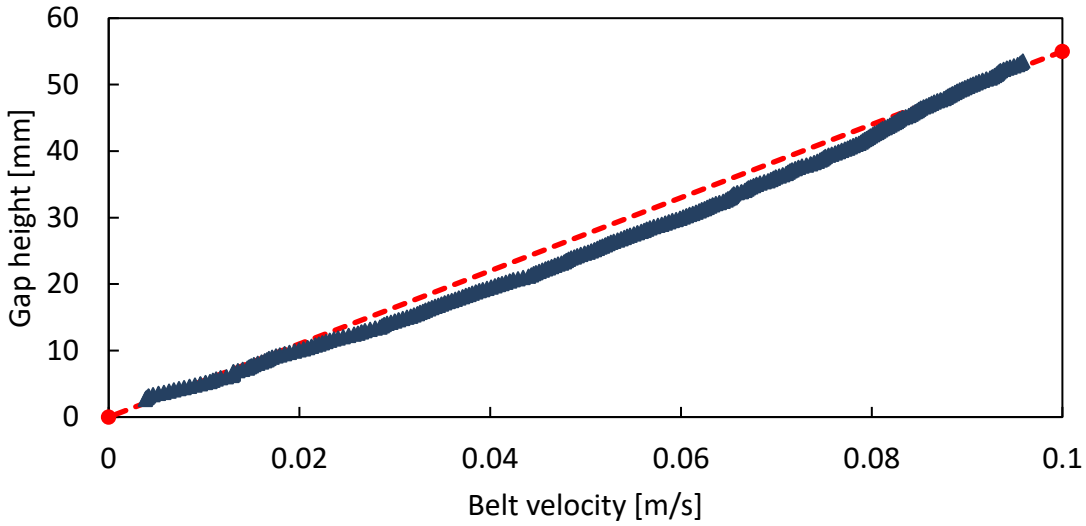


Figure 6: Velocity profile at an adjusted belt velocity of 0.1 m/s and a gap height of 55 mm in the middle of the flow channel (triangle) and ideal Couette flow (dashed line).

## Summary

We presented an experimental setup for investigating the influence of inertia on incipient particle motion in laminar shear flow. We analyzed the flow conditions by considering the critical Shields number at different locations and by detecting the flow field of the Couette flow. For a range from 12.75 cm to 142.75 cm in flow direction the standard derivation of the Shields number is 2.7 %. It was shown, that the influence of the side walls quickly diminishes so that the standard derivation from the middle of the flow channel up to 65 mm outwards is 2.6 %. The PIV measurement is in good agreement with an ideal Couette flow.

## Acknowledgement

The support from Deutsche Forschungsgemeinschaft through No. WI 2672/15-1 is gratefully acknowledged.

## Literature

**Agudo J. R., Dasilva S., Wierschem A., 2014**: “How do neighbors affect incipient particle motion in laminar shear flow?”, Phys. Fluids 26, 053303
**Agudo J. R., Han J., Park J., Kwon S., Loekman S., Luzi G., Linderberger C., Delgado A., Wierschem A., 2018**: “Visually Based Characterization of the Incipient Particle Motion in Regular Substrates: From Laminar to Turbulent Conditions”, J. Vis. Exp. 132:e57238
**Agudo J. R., Illigmann C., Luzi G., Laukart A., Delgado, A., Wierschem, A., 2017**: “Shear-induced incipient motion of a single sphere on uniform substrates at low particle Reynolds numbers”, J. Fluid Mech. 825:284-314
**Agudo J. R., Wierschem A., 2012:** “Incipient motion of a single particle on regular substrates in laminar shear flow”, Phys. Fluids 24, 093302
**Birkhofer B. H., Eischen J., Megias-Alguacil D., Fischer P., Windhab E. J.:** “Computer-Controlled Flow Cell for the study of Particle and Drop Dynamics in Shear Flow Fields”, 2005, Ind. Eng. Chem. Res., Vol. 44, pp. 6999-7009



GALA e.V., Karlsruhe, Germany, ISBN 978-3-9816764-4-0

**Bleil S., Marr D. W. M., Bechinger C., 2006:** “Field-mediated self-assembly an actuation of highly parallel microfluidic devices”, Appl. Phys. Lett. Vol. 88, p. 263515
**Burdick G. M., Berman N. S., Beaudoin S. P., 2005:** “Hydrodynamic particle removal from surfaces”, Thin Solid Films, Vol. 488, pp 116-123
**Carneiro M. V., Pähtz T., Herrmann H. J., 2011:** “Jump at the Onset of Saltation”, PRL 107, 098001
**Charru F., Larrieu E., Dupont J.-B., Zenit R., 2007**: “Motion of a particle near a rough wall in a viscous shear flow”, J. Fluid Mech., Vol 570, pp 431-453
**Charru F., Mouilleron H., Eiff O., 2004:** “Erosion and deposition of particles on a bed sheared by a viscous flow”, J. Fluid Mech. 519:55-80
**Couliou M., Monchaux R., 2015:** “Large-scale flows in transitional plane Couette flow: A key ingredient of the spot growth mechanism”, Phys. Fluids, Vol. 27, 034101
**Dakhil H., Do H., Hübner H. Wierschem A., 2018:** “Measuring the adhesion limit of fibronectin for fibroblasts with a narrow-gap rotational rheometer”, Bioprocess Biosyst. Eng., Vol. 41 p. 717-720
**Daviaud F., Hegseth J., Berge P., 1992:** “Subcritical Transition to Turbulence in Plane Couette Flow”, Physical Review Letters, Vol. 69, Number 17, pp. 2511-2516
**Derksen J. J. 2011**: “Simulations of granular bed erosion due to laminar shear flow near the critical Shields number”, Phys. Fluids 23:113303
**Deskos G., Diplas P., 2018**: “Incipient motion of a non-cohesive particle under Stokes flow conditions”, Int. J. Multiphase Flow 99:151-161
**Dey S., Ali S. Z., 2018:** “Review Article: Advances in modeling of bed particle entrainment sheared by turbulent flow”, Physics of Fluids 30, 061301
**Fan F. G., Solanti M., Ahmadi G., Hart S. C., 1997:** “Flow-induced resuspension of ridig-link fibers from surfaces”, Aerosol Sci. Technol., Vol. 27, pp. 97-115
**Groh C., Wierschem A., Aksel N., Rehberg I., Kruelle C. A., 2008:** “Barchan dunes in two dimensions: Experimental tests for minimal models“, Phys. Rev E, 78, 021304
**Kondo T., Ando K., 2019:** “Simulation of high-speed droplet impact against a dry/wet ridig wall for understanding the mechanisms of liquid jet cleaning”, Phys. Fluids, Vol 31, p. 013303
**Loiseleux T., Gondret P., Rabaud M., Doppler D., 2005**: “Onset of erosion and avalanche for an inclined granular bed sheared by a continuous laminar flow”, Phys. Fluids 17:103304
**Näger C., Wachter F., Lienhart H., Czwielong F., Riedel J., Becker S., 2023**: “Boundary layer measurements of the flow along a streamwise-oriented circular cylinder using particle tracking velocimetry”, International Journal of Heat and Fluid Flow 104, 109225
**Nguyen N. K., Yoon K. B., 2009:** “Facile organization of colloidal particles into large, perfect, one- and two-dimensional arrays by dry manual assembly on patterned substrates”, J. Am. Chem. Soc. Vol 131, pp. 14228-14230
**Olayiwola B., Walzel P., 2009:** “Effects of in-phase oscillation of retentate and filtrate crossflow filtration at low Reynolds number”, J. Membr. Sci., Vol. 345, pp. 36-46
**Seizilles G., Devauchelle O., Lajeunesse E., Metivier F., 2013**: “Width of laminar laboratory rivers”, Phys. Rev. E 87:052204
**Shields A., 1936:** “Anwendungen der Ähnlichkeitsmechanik und der Turbulenzforschung auf die Geschiebebewegung“, Mitteilung der Preußischen Versuchsanstalt für Wasserbau und Schiffbau, Vol. 26
**Stevanovic V. D., Stanojevic M. M., Jovovic A., Radic D., Petrovic M. M., Karlicic N. V., 2014**: “Analysis of transient ash pneumatic conveying over long distance and prediction of transport capacity”, Powder Technol. Vol. 254, pp. 281-290
**Taylor G. I., 1934:** “The Formation of Emulsions in Defiable Fields of Flow”, Proc. Roy. Soc., Vol. 146, Issue 858
**Tillmark N., Alfredsson H., 1992:** “Experiments on transition in plane Couette flow”, J. Fluid Mech. Vol. 235, pp. 89-102
**Topic N., Agudo J. R., Luzi G., Czech F., Wierschem A., 2022:** “Shear-induced motion of a bead on regular substrates at small particle Reynolds numbers”, J. Fluid Mech., Vol. 946, A45
**Topic N., Retzepoglu S., Wensing M., Illigmann C., Luzi G., Agudo J. R., Wierschem A., 2019**: “Effect of particle size ratio on shear induced onset of particle motion at low particle Reynolds numbers: From high shielding to roughness”, Phys. Fluids 31:063305
**White C. M., 1940:** “The equilibrium of grains on the bed of a stream”, The Royal Society, Vol. 174, Issue 958
**Wierschem A., Groh C., Rehberg I., Aksel N., Kruelle C. A., 2008:** “Ripple formation in weakly turbulent flow“, Eur. Phys. J. E 25, pp. 213-221
**Yin Y., Lu Y., Gates B., Xia Y., 2001:** “Template-assisted self-assembly: A practical route to complex aggregates of monodispersed colloids with well-defined sizes, shapes, and structures”, J. Am. Chem. Soc., Vol. 123, pp. 8718-8729

 
GALA e.V., Karlsruhe, Germany, ISBN 978-3-9816764-4-0